J. Membrane Biol. 86, 17–26 (1985)

The Journal of
Membrane Biology

A Kinetic Analysis of the Electrogenic Pump of *Chara corallina*: II. Dependence of the Pump Activity on External pH

Y. Takeuchi, U. Kishimoto, T. Ohkawa, and N. Kami-ike
Department of Biology, College of General Education, Osaka University, Toyonaka, 560 Japan

Summary. The current-voltage curve of the *Chara* membrane was obtained by applying a slow ramp de- and hyperpolarization by use of voltage clamp. By inhibiting the electrogenic pump with 50 μm DCCD (dicyclohexylcarbodiimide), the *I-V* curve approached a steady state within 100 min, which gave the i_d-V curve of the passive diffusion channel. The i_p-V curve of the electrogenic pump channel was obtained by subtracting the latter from the former. With the increase of external pH, the i_d-V curve showed only a slight change, while the i_p-V curve of the pump channel showed almost a parallel shift, in the hyperpolarizing direction, along the voltage axis in the pH range between 6.5 and 7.5. The sigmoidal i_p-V curve in this pH range could be simulated satisfactorily with the five-state model reported previously (U. Kishimoto, N. Kami-ike, Y. Takeuchi & T. Ohkawa, *J. Membrane Biol.* **80**:175–183, 1984) as well as with a lumped two-state model presented in this report. The analysis based on these models suggests that the electrogenic pump of the *Chara* membrane is mainly a $2H^+/1ATP$ pump. The forward rate constant in the voltage-dependent step increased with the increase of external pH, while the backward one decreased. On the other hand, the forward rate constant in the voltage-independent step remained almost unchanged with the increase of external pH, while the backward one increased markedly. The pump conductance at the resting membrane potential showed either a slight increase or a decrease with the increase of external pH, depending on the sample. Nevertheless, the pump current showed generally a slight increase with the increase of external pH.

Key Words *Chara* · electrogenic pump · chord conductance · *I-V* curve · kinetic model · pH dependence

Introduction

Kishimoto (1959) found a marked dependence of the membrane potential (E) of *Chara corallina* on the external pH, having a peak hyperpolarization at around pH 7. Kitasato (1968) found similar results. Moreover, he noticed that E of *Nitella clavata* was more negative than that expected from the Goldman equation. When he voltage clamped the membrane of this cell at the Nernst potential for K^+, i.e., E_K, the clamp current changed largely with the change of external pH. He interpreted this to mean that this current corresponded to the active H^+ efflux, and this caused a large passive influx of H^+ through the passive diffusion channel and thus a large hyperpolarization of E from E_K. This current was inhibited by DNP (2,4-dinitrophenol). Similar pH dependences of E have been tested in many characean species [Adrianov et al. in *Nitella mucronata* (1968); Lannoye et al. in *Chara australis* (1970); Rent et al. in *Nitella clavata* (1972); Spanswick in *Nitella translucens* (1972); Richards & Hope in *Chara corallina* (1974); Saito & Senda in *Nitella axilliformis* (1973, 1974); Keifer & Spanswick in *Chara corallina* (1978); Fujii et al. in *Chara australis* (1979); Kawamura et al., in *Chara australis* (1980); Kishimoto et al. in *Chara corallina* (1981); Tazawa & Shimmen in *Chara australis* (1980) and in *Nitellopsis obtusa* (1982)]. E is most hyperpolarized at pH around 7 or 8. The slope of change in E in these reports ranged between 30 and 55 mV/pH for the change of external pH from 6 to 8.

However, there is a great variance among the data in those reports on conductance (G) of the characean membrane and its change with pH. Richards and Hope (1974), Fujii et al. (1979), Kawamura et al. (1980) and Kishimoto et al. (1981) found that G was larger at pH_o 6 than at pH_o 8 both in the light and in the dark. In contrast, Spanswick (1972), Saito and Senda (1973, 1974), and Keifer and Spanswick (1978) found that G was smaller at pH_o 6 than at pH_o 8 in the light. The difference may be caused by the difference in culture condition.

Previously we reported an improved method for determining the conductance of the *Chara* membrane (Kishimoto et al., 1982). This method was applied to the determination of the membrane conductance at the resting state both before and after inhibition of the electrogenic pump. Also in other papers we introduced a method of analysis capable of separating the electrogenic pump from the passive diffusion channel quantitatively (Kishimoto et

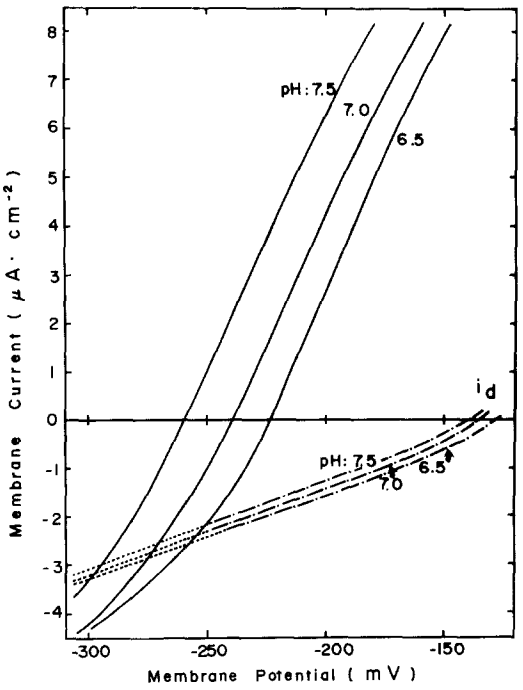

Fig. 1. Current-voltage (*I-V*) curves of the *Chara* membrane at three different external pH solutions (buffered with 2 mM TES) in the light before (full lines) and after (interrupted lines) inhibition of the electrogenic pump in the dark with 50 μM DCCD. The data is not the average of different internodes, but from a single internode. Temperature 20°C. The *I-V* curve before inhibition shifts with the increase of external pH in a direction to hyperpolarization along the *V*-axis. Note that such a shift of the i_d-*V* curve after inhibition is very small

al., 1980, 1981, 1984). We characterized the electrogenic pump with an electromotive force E_p having a conductance g_p in series.

In the present experiment the current-voltage curve of the electrogenic pump (i_p-*V* curve) was obtained by comparing the current-voltage curve (*I-V* curve) of the *Chara* membrane in the light before and after blocking the pump in the dark with DCCD (dicyclohexylcarbodiimide). With the aid of computer simulation of the i_p-*V* curve adopting a consecutive reaction kinetic model, the kinetic parameters in this model could be found. This method is applied in this report for analysis of change in activity of the electrogenic pump with external pH.

Materials and Methods

Giant internodes of *Chara corallina* were used throughout the present experiments. The internodes, which averaged 0.7 mm in diameter and 6 cm in length, were isolated from adjacent cells. Then, the internodes were kept in artificial pond water (APW) for at least two days were a photo period of 12-hr light (*ca.* 2000 lx) and 12-hr dark. The APW contained (in mM): 0.05 KCl, 0.2 NaCl, 0.1 $Ca(NO_3)_2$ and 0.1 $Mg(NO_3)_2$, and the pH was buffered at 6.5, 7.0 and 7.5 with 2 mM TES (N-Tris(hydroxymethyl) methyl-2-amino-ethane sulfonic acid). The APW was perfused at a constant rate of about 1 liter/hr. Temperature of the solution was set at about 20°C with a thermoelectric regulator (Sharp, TE-12K) and was monitored with a thermistor. The external pH was monitored with a glass pH electrode.

First, we examined the steady-state current-voltage curve (*I-V* curve) by giving step hyperpolarizations or step depolarizations of several different sizes under voltage-clamp condition (*data not shown*). Next, we recorded *I-V* curve by applying ramp hyperpolarization or ramp depolarization under voltage-clamp condition. We found these two *I-V* curves were almost the same, if we chose the ramp rate as slow as 100 mV/30 sec (Kishimoto et al., 1984). In the present experiments the current-voltage curve (*I-V* curve) was obtained by applying a ramp hyperpolarization first and a ramp depolarization next under voltage-clamp condition. One set of *I-V* curve could be obtained with this method within about one minute. Firstly, a set of *I-V* curves at different external pH's was obtained on a single internodal cell in the light (about 3000 lx) before inhibition of the pump. It was necessary to wait for 5 to 10 min before going into new steady states after pH changes. By inhibiting the electrogenic pump with 50 μM DCCD in the dark the *I-V* curve approached a steady *I-V* curve within about 100 min. The latter *I-V* curve corresponds to the i_d-*V* curve of the passive diffusion channel (Kishimoto et al., 1984). Then, another set of i_d-*V* curves at different pH was obtained on the same internodal cells. The peak level of action potential at the late stage of pump inhibition was almost the same as that before inhibition, though the recovery phase of the action potential after inhibition was slower than that before inhibition. The i_p-*V* curve of the electrogenic pump channel can be obtained by subtracting the i_d-*V* curve from the *I-V* curve so long as no qualitative changes occur during each *I-V* span. Excitation of the diffusion channel is induced by a large depolarization, while a breakdown phenomenon is induced by a large hyperpolarization. In both cases marked changes of g_d and E_d occur (Ohkawa & Kishimoto, 1974, 1977). These changes are voltage dependent. Therefore, simple subtraction of the i_d-*V* curve from the *I-V* curve including a large voltage span would result in misinterpretation of the pump mechanism. We limited the voltage span in a comparatively narrow range. The data were recorded with a floppy disk system (YE-DATA) after A/D conversion of the data of current, together with the ramp voltage and trigger pulse with a Data Acquisition System (MDAS 8D, Datel). The current and voltage data thus digitized served for later computations. Further details are described in a previous report (Kishimoto et al., 1984).

The experimentally obtained i_p-*V* curves of the electrogenic pump were sigmoidal generally and could be simulated satisfactorily with Eq. (1) in the text and in the Appendix. In this equation we have four parameters, i.e., A_1, A_2, A_3 and A_4 and the number of charge (m) carried in one cycle in the electrogenic step which is assumed equal to the stoichiometric ratio (Appendix). These are five unknowns to be determined from the experimental i_p-*V* curve. For this purpose a modified Powell's program (Powell, 1965; Kotani, 1979) of successive approximation to find the best fit of the data was adopted. Actual computation was carried out through a terminal microcomputer (PC9801E, NEC) by MELCOM in the Computer Center of Osaka University. We found that the stoichiometric ratio (m) was generally very close to 2, when the *Chara* was in a normal physiological condition and if any qualitative change did not happen during the voltage span. Therefore, in the present report we assumed $m = 2$ for the sake of simplicity in simulation. However, we do not deny that m may reduce to close to 1 on some occasions.

Results

The *Chara* cells can survive for hours in an acidic solution around pH 5 or in an alkaline solution around pH 10. Solutions outside this pH range cause qualitative changes in the electrogenic pump as well as in the passive diffusion channel (Kishimoto et al., 1981). Bisson and Walker (1980*a*, *b*) demonstrated that the *Chara* membrane became OH^- permeable at pH above 10. The effect lasted for hours even after an exchange of the external solution with a neutral one. Therefore, a careful check of the reversibility of the data in the pH experiments was needed. The data in a comparatively limited range of pH change is reported in the following.

Changes of *I-V* Curves with External pH

DCCD is known as a specific blocker of F_o, F_1-ATPase of mitochondrial inner membrane and of thylakoid in chloroplasts. It binds to one of the subunits resulting in blockage of the H^+ flux through the H^+-channel portion of the ATPase. The *I-V* curves before inhibition of the pump are compared with those at different pH's in Fig. 1. These are the data on a single internodal cell. The order of change of pH was 7 → 7.5 → 7 → 6.5 → 7. Generally we waited for 5 to 10 min in order to record the new steady-state *I-V* curve after changing external pH. We have three *I-V* curves at pH 7. These three *I-V* curves were very similar except for a slight difference in the slope, indicating reversibility in this pH-change experiment The *I-V* curve shifts in a direction to hyperpolarization along the voltage axis with the increase of external pH. This shift is almost in parallel with each other for the pH range between 6.5 and 7.5. After the inhibition of the pump with 50 μM DCCD the current-voltage curve reduces to the i_d-*V* curve of the passive diffusion channel (Kishimoto et al., 1984). The i_d-*V* curves were obtained again at pH 6.5, 7.0 and 7.5. The electromotive force (E_d) of the i_d-*V* curve does not vary much with pH between 6.5 and 7.5. Moreover, the slopes of the i_d-*V* curves for this pH range are almost the same (Fig. 1). Results of pH experiments on other single internodal cells were quite similar except for some minor differences, which will be discussed later.

Changes of i_p-*V* Curve with External pH

Since the i_d-*V* curve of the passive channel at three different pH's is known, the i_p-*V* curve of the electrogenic pump channel could be obtained by subtracting the former from the respective *I-V* curve. The i_p-*V* curve is sigmoidal in the pH range between 6.5 and 7.5. The i_p-*V* curve shifts along the voltage axis in the hyperpolarizing direction with the increase of external pH. The experimental data of the i_p-*V* curve are plotted at 5-mV intervals with symbols in Fig. 2. The voltage at which $i_p = 0$ in the i_p-*V* curve corresponds to the electromotive force E_p of the pump. The E_p hyperpolarizes with the increase of external pH. The full line in Fig. 2 is the simulated curve assuming the consecutive change of H^+-ATPase at the plasmalemma of the *Chara*. The dotted line is the chord conductance of the pump, which was calculated from the i_p-*V* curve. These are described in the following paragraphs. The maximum g_p in the i_p-*V* curve shows a slight decrease for the increase of external pH in this experiment.

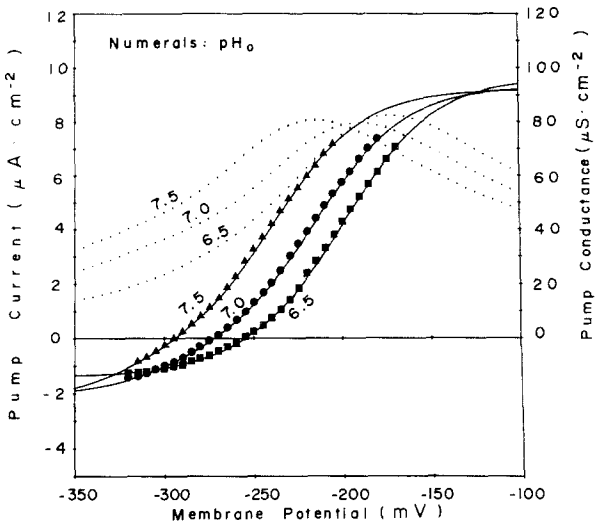

Fig. 2. i_p-*V* curves of the electrogenic pump channel of the *Chara* membrane at different external pH were obtained from three sets of current-voltage curves, i.e., *I-V* curves and i_d-*V* curves, in Fig. 1. All i_p-*V* curves are sigmoidal. The experimental data at each external pH are plotted for 5-mV intervals with symbols. The full lines are the simulated i_p-*V* curve [Eq. (1)] which is based on the kinetic reaction models shown in Fig. 3. The dotted lines are the calculated chord conductance of the electrogenic pump channel [Eq. (11) in the text]. Note that the chord conductance of the pump is voltage dependent, having a peak at a definite voltage. The i_p-*V* curves have respective reversal potential or electromotive force (E_p) at which the i_p changes its sign

Consecutive Reaction Model for the H^+-Pump

In a previous report (1984) we assumed that *m* H^+ ions were pumped out for each ATP hydrolyzed during the steady forward cyclic changes of five states of H^+-ATPase in the plasmalemma (Fig. 3*b*).

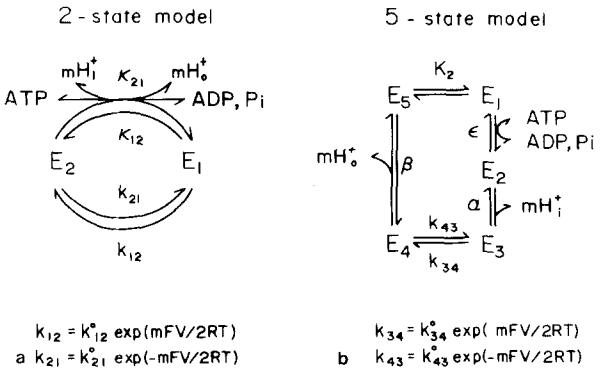

Fig. 3. Kinetic scheme for the vectorial H^+-ATPase of the electrogenic pump of the *Chara* membrane. (*a*) A lumped two-state model having four rate constants. k_{12} and k_{21} are the rate constants for the voltage-dependent (electrogenic) step and κ_{21} and κ_{12} are those for the voltage-independent step. (*b*) Successive changes of five states of the enzyme are assumed (Kishimoto et al., 1984). Coupling with ATP-hydrolysis, incorporation and release of H^+ are expressed with equilibrium constants. The forward and backward rate constants in the transition between E_5 and E_1 are assumed to be the same. These reaction steps are voltage independent. Only the step between E_3 and E_4, is assumed to be charge carrying and electrogenic. This is shown with two rate constants which are voltage dependent

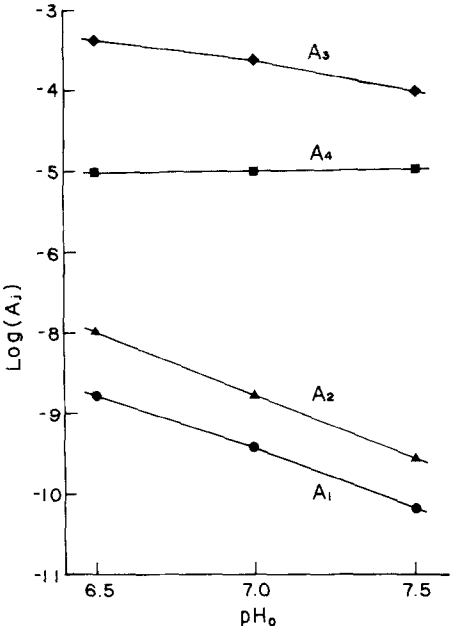

Fig. 4. Changes of four parameters (A_1, A_2, A_3 and A_4) characterizing the shape of the experimental i_p-V curve [Eq. (1)] against external pH. A_1, A_2 and A_3 decreased, while A_4 remained almost unchanged, with the increase of external pH

$E_j (j = 1, \ldots 5)$ meant the amount of each enzyme intermediate. Moreover, only a step $E_3 \leftrightarrows E_4$ was assumed to be voltage dependent and thus electrogenic. According to this model the current carried by H^+, i.e., i_p, is given by

$$i_p = (D - A_1/D)A_4/(D + A_2/D + A_3) \quad (1)$$

where $D = \exp(mFV/2RT)$, m is the stoichiometric ratio, and F, R and T have their usual meanings. Four parameters, i.e., A_1, A_2, A_3 and A_4, in Eq. (1) were functions of kinetic parameters (α, k_{34}, k_{43}, β and k_{51} (= k_{15})) in Fig. 3*b*. We had four rate constants and two equilibrium constants, which were to be evaluated. However, we have only four parameters which can be evaluated by simulating the experimental data. Thus, we needed additional assumptions such that $k_{51} = k_{15}$ and that both remained constant. General changes of the kinetic parameters during inhibition or pH change seem reasonable. Nevertheless, it involves some arbitrariness.

Hansen et al. (1981) adopted a pseudo-two-state model for the analysis of electrogenic H^+-pump and sugar-H^+ cotransport systems. In this report we adopt a similar lumped two-state model (Fig. 3*a*). We separated the electrogenic step from the nonelectrogenic step. In this simplified model we have four rate constants, i.e., k_{12}, k_{21} for the electrogenic step and κ_{21}, κ_{12} for the nonelectrogenic step. The kinetic parameters in our previous five-state model, i.e., ε, α, β, k_{51} and k_{15} are lumped together into two rate constants in the nonelectrogenic step. This lumped two-state model also gives the same i_p-V curve [Eq. (1)]. These four rate constants can be evaluated from A_1, A_2, A_3 and A_4, which are determined by simulating the experimental i_p-V curve. In this lumped two-state model the four parameters are as follows:

$$A_1 = (k^o_{21}/k^o_{12})(\kappa_{12}/\kappa_{21})([ADP][P_i]/[ATP])([H_o]/[H_i])^m \quad (2)$$

$$A_2 = k^o_{21}/k^o_{12} \quad (3)$$

$$A_3 = (\kappa_{21}[ATP][H_i]^m + \kappa_{12}[ADP][P_i][H_o]^m)/k^o_{12} \quad (4)$$

$$A_4 = mFE_o\kappa_{21}[ATP][H_i]^m \quad (5)$$

where k^o_{12} and k^o_{21} are the forward and backward rate constants, at zero membrane potential ($V = 0$), in the electrogenic step, respectively. The four rate constants can be calculated from these equations.

$$\kappa_{21} = A_4/(mFE_o[ATP][H_i]^m) \quad (6)$$

$$\kappa_{12} = \kappa_{21}(A_1/A_2)([ATP]/[ADP][P_i])([H_i]/[H_o])^m \quad (7)$$

$$k^o_{12} = (\kappa_{12}[ADP][P_i][H_o]^m + \kappa_{21}[ATP][H_i]^m)/A_3;\ k_{12} = k^o_{12}D \quad (8)$$

$$k^o_{21} = k^o_{12}A_2;\ k_{21} = k^o_{21}/D. \quad (9)$$

E_p is the voltage at which $i_p = 0$ in the i_p-V curve. E_p can be calculated from Eq. (1).

Table. Four rate constants of the electrogenic pump at different pH_o

	pH_o		
	6.5	7.0	7.5
k_{12}^o(mol^{-3} sec^{-1})	1.313×10^{10}	2.689×10^{10}	6.974×10^{10}
k_{21}^o (mol^{-3} sec^{-1})	137.1	43.8	17.9
κ_{21}(mol^{-3} sec^{-1})	2.665×10^{23}	2.582×10^{23}	2.554×10^{23}
κ_{12}(mol^{-4} sec^{-1})	6.574×10^{24}	1.005×10^{26}	1.117×10^{27}

ATP = 720 μM; ADP = 350 μM; P_i = 3 mM (Takeuchi & Kishimoto, 1983); pH_i = 7.3.

$$E_p = (RT/mF)\ln(A_1)$$
$$= (RT/mF)[\ln(k_{21}^o/k_{12}^o) + \ln(\kappa_{12}/\kappa_{21}) + \ln([ADP][P_i]/[ATP]) + m\ln([H_o]/[H_i])]. \quad (10)$$

This equation gives an explicit functional relation of E_p with H^+ concentration and also gives its absolute values, if the nucleotide concentrations and stoichiometric ratio (m) are given.

Since i_p and E_p are known, the chord conductance g_p can be calculated with,

$$g_p = i_p/(V - E_p). \quad (11)$$

The full lines in Fig. 2 are the simulated curve of the data with Eq. (1). The experimental data are plotted with symbols for 5-mV intervals. The simulation is generally satisfactory in the pH range between 6.5 and 7.5. The dotted line is the chord conductance of the pump which was calculated with Eq. (11). The chord conductance of the pump is voltage dependent having a peak at a definite voltage.

Changes of A_1, A_2, A_3 and A_4 with External pH

The four parameters, i.e., A_1, A_2, A_3 and A_4 in Eq. (1), determine the shape of the sigmoidal i_p-V curve of the pump. These could be decided by simulating the experimental i_p-V curve in Fig. 2. Changes of A_1, A_2, A_3 and A_4 of the i_p-V curve with external pH are shown in Fig. 4. A_1 decreased with the increase of external pH. A_2 decreased almost in parallel with A_1. On the other hand, A_3 decreased, while A_4 remained almost unchanged with the change in external pH. These results reflect changes with external pH of the kinetic parameters in Fig. 3.

Changes of Rate Constants of the Pump with External pH

The four rate constants in Fig. 3*a* characterize the electrogenic pump. These can be evaluated [Eqs. (6)–(9)] by use of four parameters in the preceding paragraph and are listed in the Table. The changes of the four rate constants with the change in external pH are shown in Fig. 5.

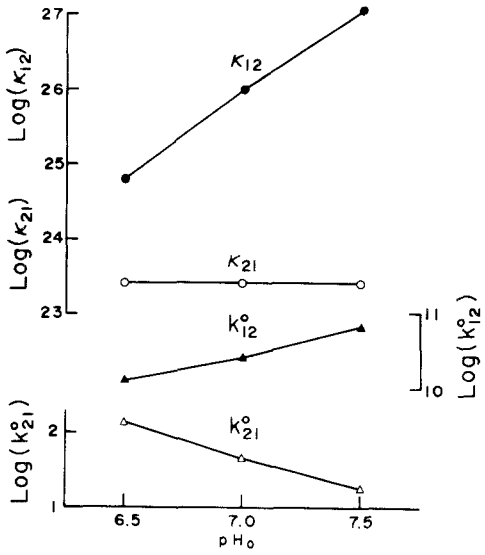

Fig. 5. Changes of four rate constants of the electrogenic pump of the *Chara* membrane with external pH. The kinetic parameters were evaluated from A_1, A_2, A_3 and A_4 in Fig. 4 with Eqs. (6)–(9) in the text. With the increase of external pH, k_{12}^o increased, while k_{21}^o decreased. On the other hand, κ_{12} increased markedly with the increase of external pH, while κ_{21} remained almost unchanged

The forward rate constant (k_{12}^o) in the electrogenic step is accelerated, while the backward one (k_{21}^o) is suppressed with the increase of external pH. On the other hand, the forward rate constant (κ_{21}) in the voltage-independent step remained almost unchanged, while the backward one (κ_{12}) increased markedly with the increase of external pH.

Changes of Fractions of Enzyme Intermediates

Our kinetic model assumes that the total number of the ATPase intermediates, i.e., E_o, remains constant and that the consecutive changes occur steadily (Appendix). In the present experiment the saturated pump current for a large depolarization is about 9 μA/cm^2. This amount is equal to $mFE_o\kappa_{21}$ ATP H_i^m [Eqs. (1) and (5)]. The peak of the pump conductance is about 80 μS/cm^2. These figures are about one-thousandth of those of the sodium channel of the squid axon membrane. Therefore, we can estimate the E_o at the plasmalemma is about 30 in each 10 μm^2; this is about one-thousandth of that reported as the density of the sodium channel in the squid giant axon membrane (Conti et al., 1975).

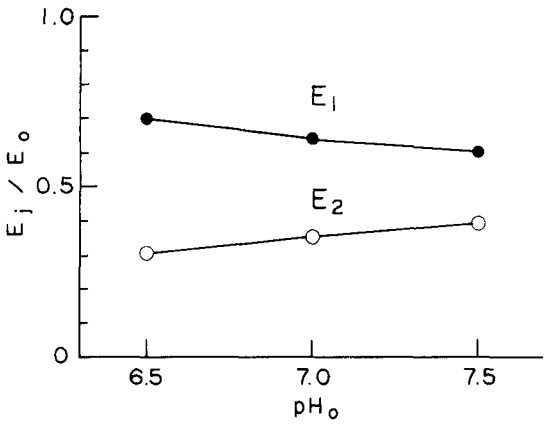

Fig. 6. Changes of fraction of each enzyme intermediate states against external pH. The fraction of E_1 decreased, while the fractions of E_2 increased, to some extent with the increase of external pH

Since the four rate constants in Fig. 3*a* are decided, the fractions of the enzyme intermediates, i.e., E_1/E_o and E_2/E_o, at the resting state for three different pH's can be calculated [Eqs. (16) and (17) in the Appendix] and are shown in Fig. 6. It is worth noting that the fraction of E_1 decreased, while E_2 increased to some extent with the increase of external pH.

Changes of Conductances and Electromotive Forces with External pH

The voltage dependences of i_p and the chord conductance g_p of the pump channel are shown in Fig. 2. The i_p and g_p at the resting potential are readable from these curves. On the other hand, the voltage dependence of i_d of the passive diffusion channel is shown in Fig. 1 and the conductances $G(= g_p + g_d)$ and g_d of the passive channel at the resting state were decided under the current-clamp condition (Kishimoto et al., 1982). These conductances, emf's and also the pump current i_p are plotted against the external pH in Fig. 7. Changes of g_d and E_d of the passive diffusion channel were negligibly small in the pH range between 6.5 and 7.5. On the other hand, the g_p of the pump channel increased to some extent, while the E_p hyperpolarized with a slope of about 40 mV/pH with the increase of external pH. According to the presented kinetic model the absolute values of E_p and its pH dependence [Eq. (10)] suggest that the stoichiometric ratio (m) of the pump is highly likely to be 2 and that the slope of E_p change is expected to be about 59 mV/pH. In some other samples we noticed that g_p decreased with the increase of external pH (Kishimoto et al., 1981). The reason for these differences will be discussed later. The pump current increased generally to some extent with external pH.

Discussion

The current-voltage curve (i_p-V curve) in the pH_o range between 6.5 and 7.5 of the electrogenic pump of the *Chara* membrane could be satisfactorily simulated (Fig. 2) with the kinetic model either with the lumped two-state model or previous five-state model which assumes two H^+ ions are released by each ATP hydrolysis (Fig. 3). In the present experiment E_p in the light hyperpolarized with a slope of about 40 mV/pH for the increase of the external pH from 6.5 to 7.5 (Fig. 7). The g_p increased to some extent with the increase of pH. In a previous report (Kishimoto et al., 1981) we showed that g_p decreased with increasing external pH. There are certainly two types of data. We noticed that the shapes of the i_p-V curve and also of the g_p-V curve were different to some extent among the internodes used. Moreover, g_p is very sensitive to the voltage change at the resting membrane potential (Fig. 2). The ratio of g_p to g_d is also different among the internodes used. These variations of conductance cause the variation of the level of the resting membrane potential among internodes and also pH dependence of g_p. Nevertheless, the overall result was the slight increase of the pump current i_p with the increase of external pH.

Beilby (1984) claims, from the experiment on a similar pH dependence of I-V curve of the *Chara* membrane, that m may be 1. We tried to find out the most probable value of m by use of the program of simulation. It gave values which are close to 2. The E_p is about -275 mV at the external pH 7. These results suggest that the electrogenic pump in the *Chara* membrane is highly likely to be a $2H^+/1ATP$ pump in a pH range between 6.5 and 7.5. However, it is probable that m may change under some physiological conditions.

If the four rate constants in our kinetic model were to remain unchanged against changes of external pH, the slope of E_p change against the external pH would be about 59 mV/pH, as expected from the kinetic model [Eq. (10)]. However, it was generally smaller than 59 mV/pH. In another pH experiment on another sample the slope of E_p was about 50 mV, while other general tendencies were very similar to the present result. In the lumped two-state model k^o_{12} (forward rate constant) in the electrogenic step increased with the increase of external pH, while k^o_{21} (backward rate constant) decreased. On the other

hand, κ_{12} (backward rate constant) in the voltage-independent step increased greatly with the increase of external pH, while κ_{21} (forward rate constant) remained almost unchanged (Fig. 5). All four rate constants in our kinetic model were not constant, but changed with the external pH_o. This suggests that some conformational change of the H^+-ATPase has occurred with the change of external pH and also that the pumping is a nonlinear mechanism. In this sense we might call these rate coefficients instead of rate constants. The H^+-ATPase in the mitochondria, chloroplasts and some bacterial membranes are regarded to be composed of several protein subunits. The H^+-ATPase of the *Chara* membrane may not be an exception. Our kinetic model is a sort of linearized one. Thus, the nonlinearity of the function of H^+-ATPase is reflected as the nonlinearity in the rate constants. According to the previous five-state model (Fig. 3*b*) the forward rate constant (k^o_{34}) in the electrogenic step increased with the external pH, while the backward one (k^o_{43}) decreased. The rate constants in the return step (k_{51} and k_{15}) were assumed to be unchanged. The equilibrium constant (α) for incorporating H^+ increased slightly with the increase of external pH, while that (β) for releasing H^+ decreased markedly (*data not shown*). The marked increase of κ_{12} in the lumped two-state model by increasing external pH seems to suggest that the rate of H^+ absorption at the external surface of H^+-ATPase increased markedly (compare marked decrease of β in the five-state model). In contrast, almost no change of κ_{21} by increasing external pH may suggest that the internal pH_i does not change appreciably with the increase of external pH. The increase of $(\kappa_{12}/\kappa_{21})$ causes a depolarization of E_p [the second term in Eq. (10)]. On the other hand, in the electrogenic step k^o_{21} decreased, while k^o_{12} increased to some extent with the increase of external pH_o. The decrease of (k^o_{21}/k^o_{12}) caused a hyperpolarization of E_p [the first term in Eq. (10)]. The extent of depolarization due to the second term in Eq. (10) is larger than the hyperpolarization due to the first term. This reduces the expected extent of hyperpolarization due to the fourth term in Eq. (10). This seems the main reason why the slope of E_p is smaller than about 59 mV/pH_o.

The role of the H^+-pump in the regulation of internal pH_i has been well recognized (Spanswick & Miller, 1977; Smith & Raven, 1979; Sanders et al., 1981; Sanders & Slayman, 1982). On the other hand, Smith and Walker (1976) and Walker (1980) demonstrated a slight increase of internal pH_i with the increase of external pH_o by measuring pH_i with DMO (5,5-dimethyl-2,4-oxazolidinedione) distribution. We tested the effect of such a possible increase of pH_i in the evaluation of four rate constants. The result was a slight increase of κ_{21} with the increase of pH_o. Three other rate constants are the same as those shown in Fig. 5 and in the Table.

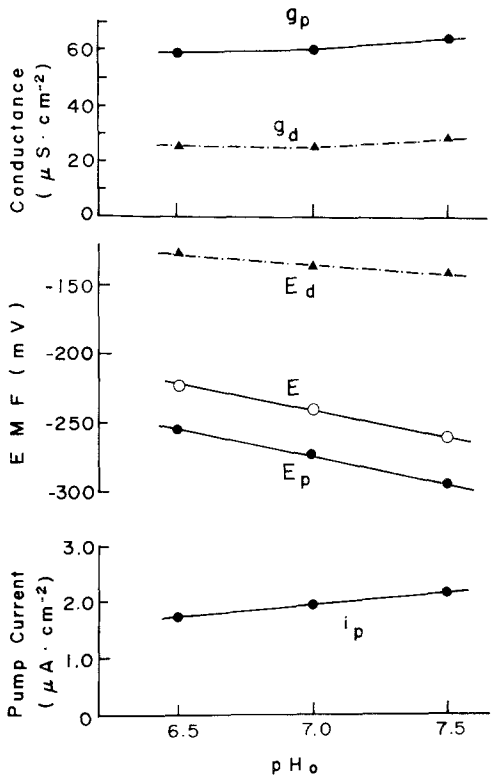

Fig. 7. Changes of conductances and electromotive forces of the passive diffusion channel and also of the electrogenic pump channel against the external pH. The conductances are generally voltage dependent. In this figure the conductances at the resting membrane potential are plotted. The conductance g_d of the passive diffusion channel was almost pH independent, while g_p of the electrogenic pump at the resting membrane potential increased slightly with the increase of the external pH for a pH range between 6.5 and 7.5. The emf (E_d) of the passive diffusion channel shifted only slightly toward a more negative level, while that (E_p) of the electrogenic pump shifted to a more negative level with a slope of about 40 mV/pH. The pump current i_p increased with the external pH in this pH range

The conductance of the passive diffusion channel was almost insensitive to the external pH change (Fig. 1). This suggests that the H^+ conductance (g_H) should be much smaller than g_K or g_{Cl}. This confirms our previous result (Kishimoto et al., 1980). Under this condition the pump current such as 0.5 to 1.0 $\mu A/cm^2$ at the resting state voltage is so large that it would exhaust almost all H^+ in the cytosol within a fraction of a second, if the electrogenic pump were a simple $2H^+/1ATP$ pump and if the supply of H^+ from the metabolism in the cytosol were not abundant enough. Some or all H^+ may

return the cell by another mechanism for the maintenance of the internal pH. A possible candidate is the H^+/anion cotransport. If the cotransport is an electroneutral one such as H^+/Cl^- or H^+/HCO^{3-} (Lucas et al. 1983), then some or all of the H^+ extruded actively can return to the cell. If such a cotransport were an electrogenic one, being coupled with the H^+-pump, the i_p-V curve would be qualitatively different from those presented in this report. So long as the cotransport is an electroneutral one, it may not affect the i_p-V curve and also may not contribute to the conductance g_d of the passive channel.

The simulation of the i_p-V curve in the moderate voltage range was almost satisfactory. However, we noticed a tendency that the experimental i_p deviated more or less in a systematic manner from the theoretical curve (Eq. 1) for a larger voltage change. This suggests some change in E_p might occur for a large depolarization or for a large hyperpolarization. In separate experiments we superimposed small step hyperpolarization pulses on the ramp voltage change (*data not shown*). The steady-state current response to this small voltage change gave the instantaneous Δi_p-Δv curve along the i_p-V curve. The change of $\Delta i_p/\Delta v$ along the i_p-V curve gave the experimental g_p, which showed a peak at the voltage close to E_p (*data not shown*). If we adopt this for g_p, E_p is expected to depolarize for a large depolarization and hyperpolarize for a large hyperpolarization. This suggests that the pH of the cytosol might have changed in proportion to the extent of large voltage change. A quantitative test for this possibility remains to be performed.

In a previous report (Kishimoto et al., 1984) we showed changes of kinetic parameters during inhibition of the pump with 50 μM DCCD. We re-examined the previous data with the lumped two-state model. The results were marked decreases of k^o_{12}, κ_{21} and κ_{12} with the progress of DCCD inhibition and almost no change in k^o_{21} (*data not shown*). These changes also describe the process of inhibition of the electrogenic pump as well as that shown with the 5-state model previously. We also tested the effect of other modification of our kinetic model (Fig. 3*b*) concerning the step for releasing ADP and/or P_i. We found that the absolute values of kinetic parameters changed depending on the model we adopted, while the general pattern of their changes was very similar. Extraction of H^+-ATPase from the plasmalemma and biochemical studies on its intermediates are certainly needed for concrete discussion of its detailed mechanism.

We are indebted to Prof. K. Kotani for introducing us to Powell's simulation program and to Ms. Y. Saegusa for her excellent secretarial assistance. This work was supported by a Research Grant from the Ministry of Education, Science and Culture of Japan.

References

Adrianov, V.K., Vorobieva, I.A., Kurella, G.A. 1968. Investigation of the resting potential of *Nitella* cells. 2. Effect of pH of medium on resting potential of *Nitella* cells. *Biophyzica* **13:**396–398

Beilby, M.J. 1984. Current-voltage characteristics of the proton pump at *Chara* plasmalemma: I. pH dependence. *J. Membrane Biol.* **81:**113–125

Bisson, M.A., Walker, N.A. 1980*a*. The hyperpolarization of the *Chara* membrane at high pH: Effects of external potassium, internal pH, and DCCD. *J. Exp. Bot.* **32:**951–971

Bisson, M.A., Walker, N.A. 1980*b*. The *Chara* plasmalemma at high pH. Electrical measurements show rapid specific passive uniport of H^+ or OH^-. *J. Membrane Biol.* **56:**1–7

Chapman, J.B., Johnson, E.A., Kootsey, J.M. 1983. Electrical and biochemical properties of an enzyme model of the sodium pump. *J. Membrane Biol.* **74:**139–153

Conti, F., De Felice, L.J., Wanke, E. 1975. Potassium and sodium ion current noise in the membrane of the squid giant axon. *J. Physiol. (London)* **248:**45–82

Fujii, S., Shimmen, T., Tazawa, M. 1979. Effect of intracellular pH on the light-induced potential change and electrogenic activity in tonoplast-free cells of *Chara australis*. *Plant Cell Physiol.* **20:**1315–1328

Hansen, U.-P., Gradmann, D., Sanders, D., Slayman, C.L. 1981. Interpretation of current-voltage relationships for "active" ion transport systems: I. Steady-state reaction-kinetic analysis of class-I mechanisms. *J. Membrane Biol.* **63:**165–190

Kawamura, G., Shimmen, T., Tazawa, M. 1980. Dependence of the membrane potential of *Chara* cells on external pH in the presence and absence of internal adenosinetriphosphate. *Planta* **149:**213–218

Keifer, D.W., Spanswick, R.M. 1978. Activity of the electrogenic pump in *Chara corallina* as inferred from measurements of the membrane potential, conductance, and potassium permeability. *Plant Physiol.* **62:**653–661

Kishimoto, U. 1959. Electrical characteristics of *Chara corallina*. *Annu. Rep. Sci. Works (Fac. Sci., Osaka University)* **7:**115–146

Kishimoto, U., Kami-ike, N., Takeuchi, Y. 1980. The role of electrogenic pump in *Chara corallina*. *J. Membrane Biol.* **55:**149–156

Kishimoto, U., Kami-ike, N., Takeuchi, Y. 1981. A quantitative expression of the electrogenic pump and its possible role in the excitation of *Chara* internodes. *In:* The Biophysical Approach to Excitable Systems. W.J. Adelman, Jr. and D.E. Goldman, editors. pp. 165–181. Plenum, New York

Kishimoto, U., Kami-ike, N., Takeuchi, Y., Ohkawa, T. 1982. An improved method for determining the ionic conductance and capacitance of the membrane of *Chara corallina*. *Plant Cell Physiol.* **23:**1041–1054

Kishimoto, U., Kami-ike, N., Takeuchi, Y., Ohkawa, T. 1984. A kinetic analysis of the electrogenic pump of *Chara corallina*: I. Inhibition of the pump by DCCD. *J. Membrane Biol.* **80:**175–183

Kitasato, H. 1968. The influence of H^+ on the membrane potential and ion fluxes of *Nitella*. *J. Gen. Physiol.* **52:**60–87

Kotani, T. 1979. A modification of Powell's method for minimization of nonlinear functions. *Computer Center News (Osaka University)* **32**:27–47

Lannoye, R.J., Tarr, S.E., Dainty, J. 1970. The effects of pH on the ionic and electric properties of the internodal cells of *Chara australis*. *J. Exp. Bot.* **21**:543–551

Läuger, P. 1979. The channel mechanism for electrogenic ion pumps. *Biochim. Biophys. Acta* **552**:143–161

Lucas, W.J., Keifer, D.W., Sanders, D. 1983. Bicarbonate transport in *Chara corallina:* Evidence for cotransport of HCO_3^- with H^+. *J. Membrane Biol.* **73**:263–274

Ohkawa, T., Kishimoto, U. 1974. The electromotive force of the *Chara* membrane during the hyperpolarizing response. *Plant Cell Physiol.* **15**:1039–1054

Ohkawa, T., Kishimoto, U. 1977. Breakdown phenomena in the *Chara* membrane. *Plant Cell Physiol.* **18**:67–80

Oosawa, F., Hayashi, S. 1983. Coupling between flagellar motor rotation and proton flux in bacteria. *J. Phys. Soc. Japan* **52**:4019–4028

Powell, M.J.D. 1965. A method of minimizing a sum of squares of nonlinear functions without calculating derivatives. *Computer J.* **7**:303–307

Rent, R.K., Johnson, R.A., Barr, C.E. 1972. Net H^+ influx in *Nitella clavata*. *J. Membrane Biol.* **7**:231–244

Richards, J.L., Hope, A.B. 1974. The role of protons in determining membrane electrical characteristics in *Chara corallina*. *J. Membrane Biol.* **16**:121–144

Saito, K., Senda, K. 1973. The effect of external pH on the membrane potential of *Nitella* and its linkage to metabolism. *Plant Cell Physiol.* **14**:1045–1052

Saito, K., Senda, K. 1974. The electrogenic ion pump revealed by the external pH effect on the membrane potential of *Nitella*. Influence of external ions and electrical current on the pH effect. *Plant Cell Physiol.* **15**:1007–1016

Sanders, D., Hansen, U-P., Slayman, C.L. 1981. Role of the plasma membrane proton pump in pH regulation in non-animal cells. *Proc. Natl. Acad. Sci. USA* **78**:5903–5907

Sanders, D., Slayman, C.L. 1982. Control of intracellular pH. *J. Gen. Physiol.* **80**:377–402

Shimmen, T., Tazawa, M. 1980. Dependency of H^+ efflux on ATP in cells of *Chara australis*. *Plant Cell Physiol.* **21**:1007–1013

Smith, F.A., Raven, J.A. 1979. Intracellular pH and its regulation. *Annu. Rev. Plant Physiol.* **35**:289–311

Smith, F.A., Walker, N.A. 1976. Chloride transport in *Chara corallina* and the electrochemical potential difference for hydrogen ions. *J. Exp. Bot.* **27**:451–459

Spanswick, R.M. 1972. Evidence for an electrogenic pump in *Nitella translucens*. I. The effects of pH, K^+, Na^+, light and temperature on the membrane potential and resistance. *Biochim. Biophys. Acta* **288**:73–89

Spanswick, R.M., Miller, A.G. 1977. Measurement of the cytoplasmic pH in *Nitella translucens*. *Plant Physiol.* **59**:664–666

Steinmetz, P.R., Anderson, O.S. 1982. Electrogenic proton transport in epithelial membranes. *J. Membrane Biol.* **65**:155–174

Takeuchi, Y., Kishimoto, U. 1983. Changes of adenine nucleotide levels in *Chara* internodes during metabolic inhibition. *Plant Cell Biol.* **2**:1401–1409

Tazawa, M., Shimmen, T. 1982. Artificial control of cytoplasmic pH and its bearing on cytoplasmic streaming, electrogenesis and excitability of *Characeae* cells. *Bot. Mag. Tokyo* **95**:147–154

Walker, N.A. 1980. The transport systems of charophyte and chlorophyte giant algae and their integration into modes of behaviour. *In:* Plant Membrane Transport: Current Conceptual Issues. R.M. Spanswick, W.J. Lucas and J. Dainty, editors. pp. 287–300. Elsevier/North-Holland, Amsterdam

Received 18 July 1984; revised 31 October 1984

Appendix

In order to discuss the voltage-dependent pump characteristics we need a kinetic analysis. Several kinetic models assuming the cyclic changes of enzyme intermediates have been proposed by several authors (Läuger, 1979; Hansen et al., 1981; Steinmetz & Anderson, 1982; Chapman et al., 1983; Oosawa & Hayashi, 1983; Kishimoto et al., 1984). In a previous report (1984) we assumed a cyclic change of five states of H^+-ATPase in the plasmalemma of *Chara*. In this model we had six kinetic parameters, i.e., four rate constants and two equilibrium constants. These were to be evaluated from four parameters (A_1, A_2, A_3 and A_4), which were determined by simulating the experimental i_p-V curve. For this purpose we had additional assumptions such as $k_{51} = k_{15}$ and that these remain constant. Changes of these kinetic parameters during DCCD poisoning showed some interesting features about the H^+-pump. However, without validating these assumptions our analysis remains qualitative.

An alternative is to adopt a lumped two-state model, which was described by Hansen et al. (1982). In this model the voltage-dependent step is expressed with two rate constants, i.e., k_{12} (forward) and k_{21} (backward) which are voltage dependent (Fig. 3*a*). The voltage-independent step is also expressed with two rate constants, i.e., κ_{21} (forward) and κ_{12} (backward) which are not voltage dependent. On the other hand, the voltage-dependent step in the previous five-state model is $E_3 \rightleftharpoons E_4$ (Fig. 3*b*) and the voltage-independent step includes $E_4 \rightleftharpoons E_5 \rightleftharpoons E_1 \rightleftharpoons E_2 \rightleftharpoons E_3$. Therefore, two equilibrium constants, α and β, and two rate constants, k_{51} and k_{15}, in the five-state model, are lumped into two rate constants, κ_{12} and κ_{21}, in the lumped two-state model. We assume that efflux or influx of H^+ occurs by the steady cyclic change of enzyme intermediates, that is, $E_1 \rightleftharpoons E_2 \rightleftharpoons E_1$, and so on. The transition rate of the enzyme from E_1 into E_2 in the voltage-dependent step is given by

$$f_{12} = k_{12}E_1 - k_{21}E_2 \tag{12}$$

where E_1 and E_2 are numbers of E_1 and E_2, respectively. These abbreviations are used hereafter. For further simplicity a symmetry in the energy barriers for the forward and backward transition in this step is also assumed (Läuger, 1979). Then,

$$k_{12} = k_{12}^o \exp(mFV/2RT);\ k_{21} = k_{21}^o \exp(-mFV/2RT) \tag{13}$$

$$f_{12} = k_{12}^o \exp(mFV/2RT)\, E_1 - k_{21}^o \exp(-mFV/2RT)E_2. \tag{14}$$

The transition rate of the enzyme from E_2 into E_1 in the voltage-independent step is given by

$$f_{21} = \kappa_{21}[\mathrm{ATP}][\mathrm{H}_i]^m E_2 - \kappa_{12}[\mathrm{ADP}][\mathrm{P_i}][\mathrm{H}_o]^m E_1. \quad (15)$$

At steady state f_{12} should be equal to f_{21}. Total amount of enzyme E_o is assumed to remain constant. By use of these two conditions the number of enzyme intermediate can be calculated.

$$E_1 = (k^o_{21}/D + \kappa_{21}[\mathrm{ATP}][\mathrm{H}_i]^m)E_o/W \quad (16)$$

$$E_2 = (k^o_{12}D + \kappa_{12}[\mathrm{ADP}][\mathrm{P_i}][\mathrm{H}_o]^m)E_o/W \quad (17)$$

where $D = \exp(mFV/2RT)$ and

$$W = k^o_{12}D + k^o_{21}/D + \kappa_{21}[\mathrm{ATP}][\mathrm{H}_i]^m + \kappa_{12}[\mathrm{ADP}][\mathrm{P_i}][\mathrm{H}_o]^m.$$

The current carried by H^+, i.e., i_p (pump current) is proportional to f_{12} ($= f_{21}$). Then, i_p can be calculated with Eqs. (12)–(17):

$$i_p = (D - A_1/D)A_4/(D + A_2/D + A_3) \quad (1)$$

where

$$A_1 = (k^o_{21}/k^o_{12})(\kappa_{12}/\kappa_{21})([\mathrm{ADP}][\mathrm{P_i}]/[\mathrm{ATP}])([\mathrm{H}_o]/[\mathrm{H}_i])^m \quad (2)$$

$$A_2 = k^o_{21}/k^o_{12} \quad (3)$$

$$A_3 = (\kappa_{21}[\mathrm{ATP}][\mathrm{H}_i]^m + \kappa_{12}[\mathrm{ADP}][\mathrm{P_i}][\mathrm{H}_o]^m)/k^o_{12} \quad (4)$$

$$A_4 = mFE_o\kappa_{21}[\mathrm{ATP}][\mathrm{H}_i]^m. \quad (5)$$

Functional shape of the pump current is expressed with Eq. (1). This equation in the lumped two-state model is just the same as that in the five-state model which was described in a previous report (Kishimoto et al., 1984). However, calculated values of kinetic rate constants depend on the model we adopt.

Previously we reported on the changes of internal adenine nucleotide levels in the *Chara* internodes during metabolic inhibition (Takeuchi & Kishimoto, 1983). According to this report, the internal concentrations of ATP, ADP and P_i of the *Chara* in the light are 0.7, 0.35 and 3.0 mM, respectively. Since [ATP], [ADP] and [P_i] are known, the four rate constants in the presented two-state model (Fig. 3*a*) can be calculated with Eqs. (2)–(5):

$$\kappa_{21} = A_4/(mFE_o[\mathrm{ATP}][\mathrm{H}_i]^m) \quad (6)$$

$$\kappa_{12} = \kappa_{21}(A_1/A_2)([\mathrm{ATP}]/[\mathrm{ADP}][\mathrm{P_i}])([\mathrm{H}_i]/[\mathrm{H}_o])^m \quad (7)$$

$$k^o_{12} = (\kappa_{21}[\mathrm{ATP}][\mathrm{H}_i]^m + \kappa_{12}[\mathrm{ADP}][\mathrm{P_i}][\mathrm{H}_o]^m)A_3;\ k_{12} = k^o_{12}D \quad (8)$$

$$k^o_{21} = k^o_{12}A_2;\ k_{21} = k^o_{21}/D. \quad (9)$$

E_p is calculated as the voltage where $i_p = 0$.

$$\begin{aligned} E_p &= (RT/mF)\ln(A_1) \\ &= (RT/mF)\,[\ln(k^o_{21}/k^o_{12}) + \ln(\kappa_{12}/\kappa_{21}) \\ &\quad + \ln([\mathrm{ADP}][\mathrm{P_i}]/[\mathrm{ATP}]) + m\ln([\mathrm{H}_o]/[\mathrm{H}_i])]. \end{aligned} \quad (10)$$

The conductance of the pump channel, i.e., g_p, is calculated as the chord conductance in our kinetic model.

$$g_p = i_p(V - E_p). \quad (11)$$

The merit of using chord conductance instead of slope conductance for the electrogenic pump is described in a previous report (Kishimoto et al., 1984).